A noninvasive method to estimate arterial impedance by means of assessment of local diameter change and the local center-line blood flow velocity using ultrasound

ELSEVIER

Ultrasound in Med. & Biol., Vol. 22, No. 7, pp. 895–905, 1996

0301-5629/96 $15.00 + .00

PII: S0301-5629(96)00082-8

●*Original Contribution*

A NONINVASIVE METHOD TO ESTIMATE ARTERIAL IMPEDANCE BY MEANS OF ASSESSMENT OF LOCAL DIAMETER CHANGE AND THE LOCAL CENTER-LINE BLOOD FLOW VELOCITY USING ULTRASOUND

PETER J. BRANDS,[†] A. P. G. HOEKS,[†] M. C. M. RUTTEN[‡] and R. S. RENEMAN*

[†]Department of Biophysics, Cardiovascular Research Institute of Maastricht, University of Limburg, Maastricht, The Netherlands; [‡]Department of Mechanical Engineering, Eindhoven University of Technology, The Netherlands; and *Department of Physiology, Cardiovascular Research Institute of Maastricht, University of Limburg, Maastricht, The Netherlands

(*Received* 9 *November* 1995; *in final form* 11 *March* 1996)

Abstract—Vascular impedance is defined as the ratio between the frequency components of the local blood pressure waveform and those of the local blood volume flow waveform. Assessment of vascular impedance is, for example, important to study heart load and distal vascular bed vasomotricity. However, only a few studies on vascular impedance have been performed in humans because pulsatile pressure and volume flow waveforms, simultaneously recorded at the same location, are difficult to obtain noninvasively. The noninvasive assessment of arterial impedance as described in this study is based on the replacement of the pressure waveform by the distension (change in diameter) waveform and the volume flow waveform by the center-line blood flow velocity waveform. Both waveforms can simultaneously and accurately be assessed by means of pulsed ultrasound. It will be shown that, depending on the Womersley number, the volume flow waveform may be replaced by the center-line blood flow velocity waveform for a given frequency range and that the pressure waveform may be replaced by the distension waveform for a wide frequency range. The validation of the proposed ultrasound method was performed through an *in vitro* study in a flow model with a distensible tube terminated with a hydraulic load (modified windkessel model). It is shown that, *in vitro,* the proposed method gives the same results as the local spectral pressure–flow relationship.

Key Words: **Pulsed ultrasound, RF cross-correlation, Signal processing, Vascular impedance, Vessel wall displacement.**

INTRODUCTION

Vascular impedance describes the spectral relationship between blood pressure and blood volume flow of an artery and characterizes the properties of the vascular bed downstream. This property makes vascular impedance of particular value in the studies on heart load, vascular circulation and distal vascular beds' vasomotricity (Adamson et al. 1990; Arbeille et al. 1995; Maulik et al. 1989; Milnor 1975; O'Rourke 1982; O'Rourke and Taylor 1967; Powalowski 1989; Westerhof and Elzinga 1974; Westerhof and Noordergraaf 1970). The information about vascular impedance presently available is based mainly on invasive measurements in animals (Attinger et al. 1966; Farrar et al. 1978; Gow and Taylor 1968; Randall and Stacey 1956), because studies on vascular impedance in humans are hampered by the lack of reliable noninvasive techniques to record pressure waveforms locally. To overcome this limitation the local distension (change in diameter) waveform will be used as a substitute for the local blood pressure waveform, while the local center-line blood flow velocity waveform is used as a substitute for the local blood volume flow waveform. Both waveforms can simultaneously and accurately be assessed by means of pulsed ultrasound. The ratio of the spectral components of the normalized distension waveform and the normalized center-line blood flow velocity waveform provides an estimate of dimensionless arterial impedance (ultrasound arterial impedance). Normalization with respect to peak-to-peak excursions within a cardiac cycle (Fig. 1) is used because then no assumptions have to be made for the conversion of the distension

Address correspondence to: Peter J. Brands, Department of Biophysics, CARIM, University of Limburg, PO Box 616, 6200 MD Maastricht, The Netherlands.

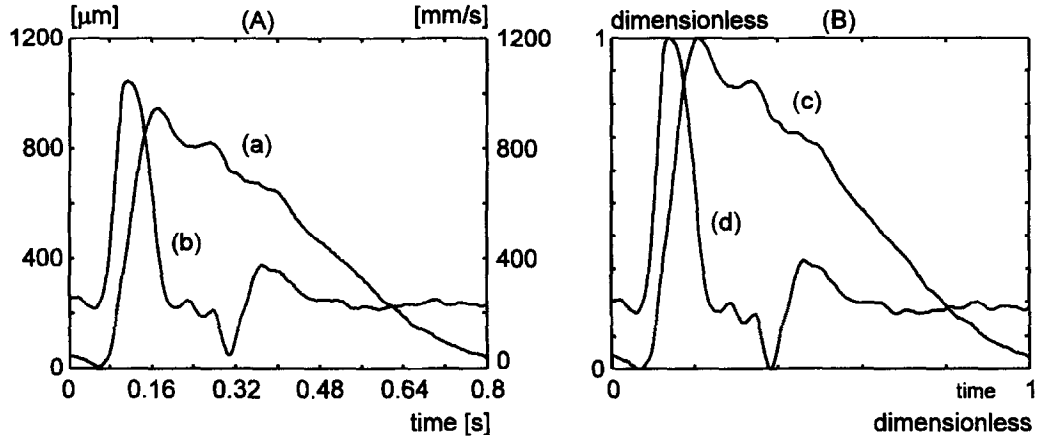

Fig. 1. (A) The distension (in microns) (a) and center-line blood flow velocity (in millimeters per second) (b) measured in the common carotid artery. (B) The normalized distension (c) and the normalized center-line blood flow velocity (d).

waveform in absolute units of pressure (millimeters of mercury) and for the conversion of the center-line blood flow velocity in absolute units of flow (liters per minute), both as function of time (Powalowski 1989). The consequence of this approach is that the ultrasound arterial impedance obtained is dimensionless and that the shape of distension and center-line blood flow velocity waveforms are considered rather than the incidental magnitude of these waveforms.

The ultrasound signal processing necessary for the assessment of the local distension waveform and the local center-line blood flow velocity waveform is performed in the RF domain and consists of a mean frequency estimator based on an RF cross-correlation model (CCM) (De Jong et al. 1990; Hoeks et al. 1993), preceded by a static discrimination filter. The ultrasound system to assess vascular impedance consists of an ultrasound echo system (operating at an emission frequency of 6.1 MHz), a data acquisition system to digitize and store the ultrasound RF signals received during a few seconds (1–4 s) as an RF matrix and a computer system to estimate off-line the dimensionless vascular impedance.

The proposed method is validated in an *in vitro* study comparing the dimensionless ultrasound vascular impedance with the dimensionless spectral relationship between local pressure and local volume flow (reference vascular impedance). The waveforms are obtained in a distensible tube terminated with a hydraulic load (modified windkessel model) under nonstationary flow conditions in which the flow wave resembles the aortic volume flow wave.

METHOD OF MEASUREMENT

Ultrasound arterial impedance assessment

Vascular impedance Z is determined in the frequency domain from successive harmonics h of pressure and volume flow waveforms over a cardiac cycle as:

$$Z(h \cdot f_0) = \frac{P(h \cdot f_0)}{Q(h \cdot f_0)} = A(h \cdot f_0) \cdot \exp(\phi(h \cdot f_0)) \qquad h = 0, 1, 2 \cdots H \quad (1)$$

where f_0 is the fundamental frequency ($h = 1$) of a given heart beat, $P(h \cdot f_0)$ the harmonics of the blood pressure waveform, $Q(h \cdot f_0)$ the harmonics of the blood volume flow waveform, and $A(h \cdot f_0)$ the magnitude and $\phi(h \cdot f_0)$ the phase of the vascular impedance, respectively. If $h = 0$, the ratio of mean blood pressure and mean blood volume flow is computed, giving the peripheral resistance.

The method to noninvasively determine arterial impedance as presented in this article is based on the assessment of the ratio of the harmonics of the normalized change in diameter waveform during the cardiac cycle $\Delta d(t)$ and the harmonics of the normalized center-line mean blood flow velocity waveform during the cardiac cycle $\overline{v}(t)$ as:

$$Z_{DV}(h \cdot f_0) = \frac{D_n(h \cdot f_0)}{V_n(h \cdot f_0)} = A_n(h \cdot f_0) \cdot \exp(\phi(h \cdot f_0)) \qquad h = 0, 1, 2 \cdots H \quad (2)$$

where Z_{DV} is the dimensionless ultrasound vascular impedance, $A_n(h \cdot f_0)$ its magnitude and $\phi(h \cdot f_0)$ its phase. Replacement of the volume flow waveform by the center-line flow velocity waveform and the pressure waveform by the distension waveform assumes a linear relationship between the related parameters. As will be demonstrated, this linear relationship is an ac-

ceptable assumption for elastic arteries like the common carotid artery.

Data acquisition

The measurement system for the ultrasound arterial impedance consists of an ultrasound echo system, a data acquisition system to store the ultrasound information received during a few seconds (1–4 s) and a computer system to estimate off-line the dimensionless arterial impedance. The echo system is connected to the acquisition system by the following three signals: (1) the RF signal after amplification and bandpass filtering according to the quality factor of the ultrasound transducer used; (2) a trigger to indicate the moment of ultrasound emission; and (3) a sample clock synchronous with the emission trigger. The latter is necessary to retain the phase information in the sampled RF signals. Considering the quality factor Q (Q = mean frequency/bandwidth) of the ultrasound transducer, a sample frequency of three or four times the emission frequency is adequate to capture all the available signal information. The echo system connected to the acquisition system should have a pulse repetition frequency (PRF) of ultrasound bursts in echo M-mode in accordance with the anticipated maximum blood flow velocities (up to 10 kHz).

The RF signals acquired in M-mode are stored as an RF matrix organized in time and as three regions in depth: (1) 64 RF sample points of the anterior vessel wall reflection; (2) 32 RF sample points in the center of the lumen of the blood vessel; and (3) 64 RF sample points of the posterior vessel wall reflection (Fig. 2). The reason for using these three specified regions rather than a continuous single depth range is to reduce the amount of RF data to be stored. Moreover, only the distension and center-line blood flow velocity waveforms are relevant to obtain an estimate of the dimensionless ultrasound vascular impedance. The echo system is operated in M-mode to retain a high axial resolution. This does not conflict with velocity estimation because of the RF-processing employed. The temporary storage of the acquired RF-signals has the advantage that the RF matrix (Fig. 2) can be retained on a backup medium (DAT or WORM-CD) for further off-line analysis.

The acquisition system samples and stores the RF-signals in real-time in the internal memory of the computer system. It has an external sample frequency of 24.4 MHz (sample clock provided by the attached echo system), a dynamic range of 72 dB (12 bit) and is connected to the computer system through a VESA-local bus. The latter is required to achieve a high data throughput rate (up to 10 Mbyte/s) to the internal memory of the computer system. For the dimensionless vascular impedance measurements, the acquisition memory is organized as 32,768 temporal RF signals of 160 spatial sample points each (64 anterior, 64 posterior and 32 lumen center sample points), requiring an acquisition memory size of 10 Mbyte. At a PRF of 8 kHz, 32,768 temporal RF signals are equivalent to 4 s. Thus, the RF matrix (Fig. 2) consists of 4 s of temporal and 5 mm of spatial ultrasound information (2 mm from the anterior and posterior vessel wall together with 1 mm from the center of the lumen).

To select the relevant RF samples and to restrict user interference, an automatic method rather than a

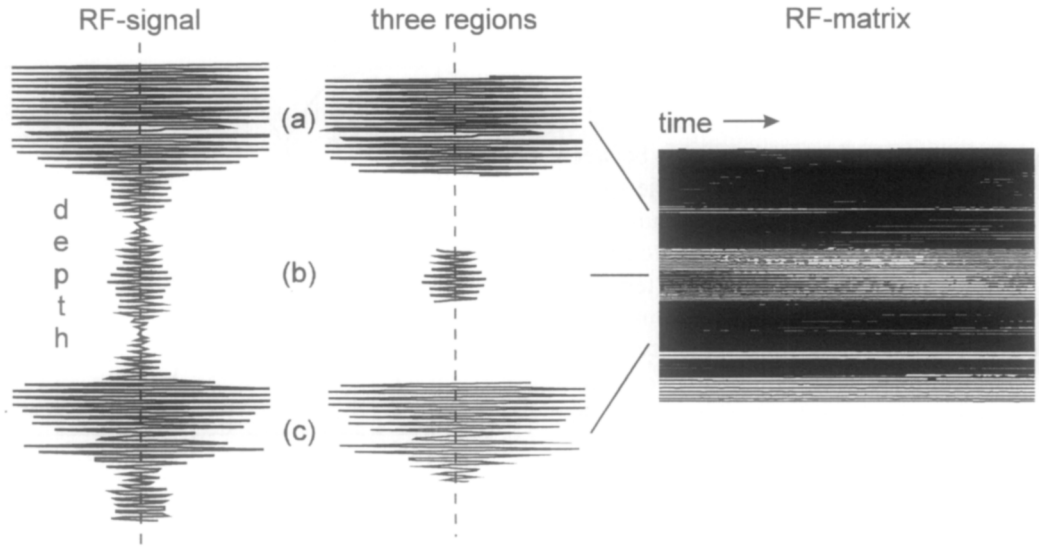

Fig. 2. Data storage of the acquired RF signals in an RF matrix as a function of time from three regions in depth: (a) anterior vessel wall; (b) center of the lumen; and (c) posterior vessel wall.

manual positioning procedure is used to identify the wall–lumen interface (Hoeks et al. 1995). The identification of the lumen of a blood vessel by the user activates data acquisition which starts synchronously with a trigger derived from the R-wave of an ECG signal. The identification of the lumen, based on the envelope of the RF signals, is necessary for the automatic detection of the wall–lumen interface synchronously with the start of data acquisition. The method is based on the generation of dynamically adjusting threshold levels, independent for both vessel walls, using attack–sustain lowpass filters with a response time on the order of the response time of the depth-dependent gain control (approximately 10 μs). The accuracy and reproducibility of the automatic detection has been verified. The verification results show that the proposed method is consistent with a standard deviation of half the resolution of the attached echo system.

Mean frequency estimation

The distension and center-line blood flow velocity waveforms are assessed with the RF domain CCM estimator (De Jong et al. 1990; Hoeks et al. 1993) because of its high quality for wide-bandwidth RF signals. The estimated dimensionless velocity, $\hat{\varphi}_s$, of the scattered signal and the dimensionless velocity, $\hat{\varphi}_r$, of the reflected signal are related to the center-line mean blood flow velocity and the velocity of vessel wall displacement as:

$$\hat{v} = \frac{c}{2 \cdot \cos \alpha} \cdot \frac{PRF}{f_{s-rf}} \cdot \hat{\varphi} \qquad (3)$$

where c is the speed of sound, PRF is the pulse repetition frequency, f_{s-rf} is the spatial sample frequency and α the observed angle between the ultrasound beam and the blood vessel axis. Vessel wall motion is obtained from the integrated vessel wall velocity on a beat-to-beat basis. The distension waveform as function of time is obtained from the difference in motion between the anterior and the posterior vessel walls. The spatial estimation window length of the CCM estimator is selected according to the length of the emitted ultrasound burst (two wavelengths), while the temporal estimation window length is selected according to the temporal behavior of the blood flow velocity. For a 6.1-MHz pulsed-echo system emitting two wavelengths, the spatial estimation window is set at eight spatial sample points, *i.e.*, 250 μm at a sample frequency of 24.4 MHz. A temporal estimation window of 10 ms (80 temporal sample points at a PRF of 8 kHz) ensures a low standard deviation of the velocity estimate, whereas it does not compromise the temporal behavior of the observed velocities.

Discrimination filter

Discrimination between the reflected signals and the scattered signals in the RF matrix acquired (Fig. 2) is obtained by means of a static discrimination filter. The characteristics of such a filter are based on general assumptions of the frequency characteristics of the reverberations and the reflected signal; *i.e.*, a low frequency, a narrow bandwidth and a high amplitude. The low-pass filtration to remove noise and scattered signals from the RF signals received is obtained with a second order IIR low-pass filter (LPF). The cut-off frequency of the LPF is based on the assumed maximum velocity of vessel wall motion (10 mm/s) and set at 40 Hz (Fig. 3). The high-pass filtration to remove the reflected signals is obtained with a second order IIR high-pass filter (HPF). The cut-off frequency of the HPF is set at 100 Hz in accordance with the temporal length of the estimation window (10 ms) (Fig. 3). The difference in amplitude between the reverberations in the center of the lumen and the scattered signal is on the order of 20 dB. A suppression of 20 dB for a second order HPF (roll-off of 12 dB/octave) with a cut-off frequency of 100 Hz is achieved at frequencies lower than 32 Hz.

Postprocessing

Postprocessing of vessel wall motion involves a moving average filter with a five-sample-point line kernel acting on half overlapping sample windows spaced at 5 ms, giving a response time of 25 ms (40 Hz). The postprocessing of the dimensionless velocity is carried out by means of a signal-to-noise ratio (SNR) decision rule (Brands et al. 1995), a

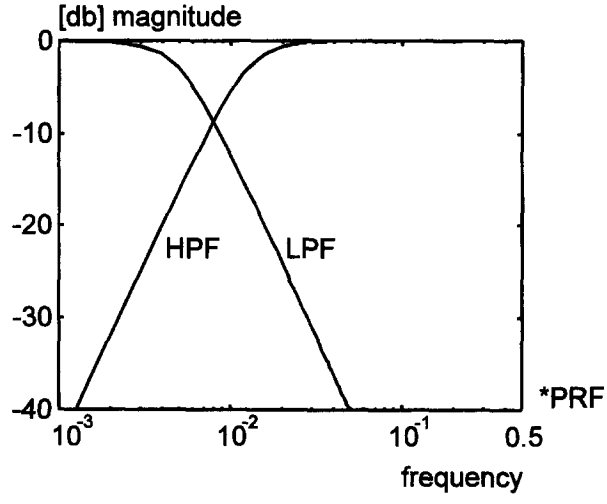

Fig. 3. The transfer function of the static discrimination filter used to estimate distension and velocity to compute vascular impedance.

median filter and a moving average filter. To reduce the variation of the estimated SNR_S (CCM estimator) of the scattered signal, this $\hat{SNR}_S$ is subjected to a moving average filter with a five-sample-point line kernel (25-ms response). If the smoothed $\hat{SNR}_S$ is less than −3 dB ($\hat{SNR}_S < 0.5$), it may be expected that the estimation window does not contain a scattered signal and the corresponding estimate of the dimensionless velocity, $\hat{\varphi}_s$, is set at zero. To remove possible false positive and false negative decisions inducing spot noise, $\hat{\varphi}_s$ is subjected to a median filter with a five-sample-point line kernel. Furthermore, $\hat{\varphi}_s$ is subjected to an averaging filter, with a five-sample-point line kernel, to remove the quantization noise introduced by the median filter. Finally $\hat{\varphi}_s$ is converted to an index of blood flow velocity (Fig. 4).

Summary

The entire ultrasound signal processing procedure to estimate simultaneously distension and center-line blood flow velocity waveform consists of:

1. Identification of the vessel lumen boundary to distinguish three regions in depth and to store these signals in an RF matrix (Fig. 2).
2. Discrimination with a static discrimination filter.
3. Estimation of the dimensionless velocities, $\hat{\varphi}_r$ and $\hat{\varphi}_s$, of the reflected and the scattered signal, respectively, together with the SNR of the scattered signal.
4. Postprocessing of the dimensionless velocity, $\hat{\varphi}_s$, of the scattered signal and of the integrated dimensionless velocity, $\hat{\varphi}_r$ (vessel wall motion).
5. Conversion of $\hat{\varphi}_s$ and vessel wall motion to blood flow velocity and distension, respectively.

To reduce the computational load, processing steps 2 and 3 are performed in a temporal recursive way.

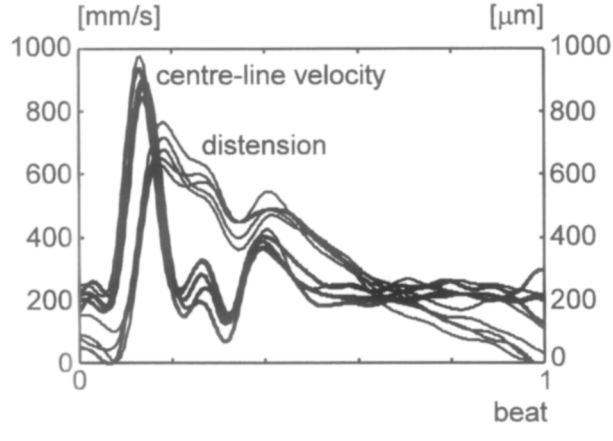

Fig. 4. Estimated distension and center-line blood flow velocity waveforms over four heart beats measured in the common carotid artery.

DIMENSIONLESS VASCULAR IMPEDANCE

From the equation of motion of a Newtonian fluid through a linearly elastic and isotropic tube, the center-line blood flow velocity can be derived. The latter shows that, depending on the Womersley number, the center-line blood flow velocity waveform is almost linear with volume flow for a given frequency range. From the force equilibrium of a tube, it follows that distension is linear with pressure and that this linearity is not frequency dependent.

Relation volume flow and center-line flow velocity

From the Navier–Stokes equations coupled with the equilibrium equations of the tube, the center-line blood flow velocity may be derived. This theory is applicable when harmonic solutions for pressure and volume flow are considered only and if the flow velocity is low in comparison with the pulse wave velocity (Womersley 1957). The Navier–Stokes equations will, under these assumptions, reduce to:

$$\rho \cdot \frac{\delta v_x}{\delta t} = -\frac{\delta p}{\delta x} + \eta \frac{\delta}{\delta r}\left(\frac{\delta v_x}{\delta r}\right) \qquad (4)$$

where η [Pa·s] is the dynamic viscosity, ρ is the specific mass of the fluid, v_x the axial velocity component at the radial position r and $\delta p/\delta x$ the axial pressure gradient. An analytical solution for the harmonics h of the axial velocity profile $v_x(h,r,t)$ can be derived as:

$$v_x(h,r,t) = RE\left(\frac{R^2}{j\cdot\eta\cdot\alpha_h^2}\left[1 - \frac{J_0(\alpha_h\cdot j^{3/2}\cdot r/R)}{J_0(\alpha_h\cdot j^{3/2})}\right] \times \frac{\delta p(h,t)}{\delta x}\right) \quad h \geq 1 \qquad (5)$$

where $\delta p(h,t)/\delta x$ is the hth harmonic of the axial pressure gradient, R is the mean radius of the tube, J_0 is the Bessel function of the first kind of order zero, ω_0 is the angular frequency of a heart beat, RE is the real part operator and α_h is the Womersley number defined as:

$$\alpha_h = R\cdot\sqrt{h\cdot\omega_0\cdot\frac{\rho}{\eta}} \qquad (6)$$

Integration of eqn (5) over the vessel radius yields the relation between the harmonics of the local volume flow, $Q(h,t)$, and the harmonics of the axial center-line flow velocity $v_x(h,r,t)_{r=0}$ as:

$$v_x(h,r,t)_{r=0} = RE\left(\frac{1}{1 - F_{10}(\alpha_h)}\right)\cdot\frac{Q(h,t)}{\pi\cdot R^2} \quad (7)$$

with the Womersley function, $F_{10}(\alpha_h)$, defined as:

$$F_{10}(\alpha_h) = \frac{2\cdot J_1(j^{3/2}\cdot\alpha_h)}{j^{3/2}\cdot\alpha_h\cdot J_0(j^{3/2}\cdot\alpha_h)} \quad (8)$$

where J_1 is the Bessel function of the first kind order one. From the volume flow center-line flow velocity eqn (7) it follows that, if $1/(1 - F_{10}(\alpha_h))$ may be linearized for a given range of the Womersley number, α_h, the center-line blood flow velocity, is almost linearly dependent on the flow, Q, in that frequency range. In Fig. 5, it is shown that for a Womersley number α_1 of the order of five, which is a realistic value for the carotid artery (see Fig. 5a), linearization of the function $1/(1 - F_{10}(\alpha_h))$ is possible. The signal power of the distension and center-line blood flow velocity is concentrated in the lower harmonics (Fig. 6). Therefore, the linearization of the function $1/(1 - F_{10}(\alpha_h))$ is applied to the part of the spectrum between the second and the fifth harmonic.

Relation between local pressure and distension waveform

The distension waveform of the vessel wall is obtained from the integrated velocities of the anterior and posterior wall displacements. From the equilibrium equation of a tube with radius R, wall thickness h and pressurized with pressure p, the pressure–distension relation can be derived. This equation is based on the force equilibrium between pressure × radius and wall thickness × circumferential stress $\sigma_{\varphi\varphi}$ as:

$$h\sigma_{\varphi\varphi} = p\cdot R \quad (9)$$

The circumferential stress for a linearly (visco)elastic thin-walled tube is defined as:

$$\sigma_{\varphi\varphi} = \frac{E(\omega)\cdot\epsilon_{\varphi\varphi}}{1 - \nu^2} \quad (10)$$

where $\epsilon_{\varphi\varphi}$ is the strain and E and υ the (complex) Young's modulus and the Poisson ratio of the material, respectively. The strain in the circumferential direction is defined as:

$$\epsilon_{\varphi\varphi} = \frac{u_r}{\bar{R}} \quad (11)$$

with u_r the radial wall displacement and $\bar{R}$ the mean vessel radius. The pressure–distension relation then reads:

$$u_r = \frac{\bar{R}^2(1 - \nu^2)}{hE(\omega)}p = g(\omega)\cdot p \quad (12)$$

The pressure–distension relation is a function of frequency $g(\omega)$ due to viscoelastic effects in the vessel wall. However, when the imaginary part of the Young's modulus, E, of the vessel material is small compared to the real part, the radial wall displacement is linear with pressure and not very frequency dependent. For blood vessels, this is indeed the case (Milnor 1989; Westerhof and Noordergraaf 1970).

IN VITRO VALIDATION

Experimental setup

The validation of the method proposed to estimate dimensionless vascular impedance using pulsed ultra-

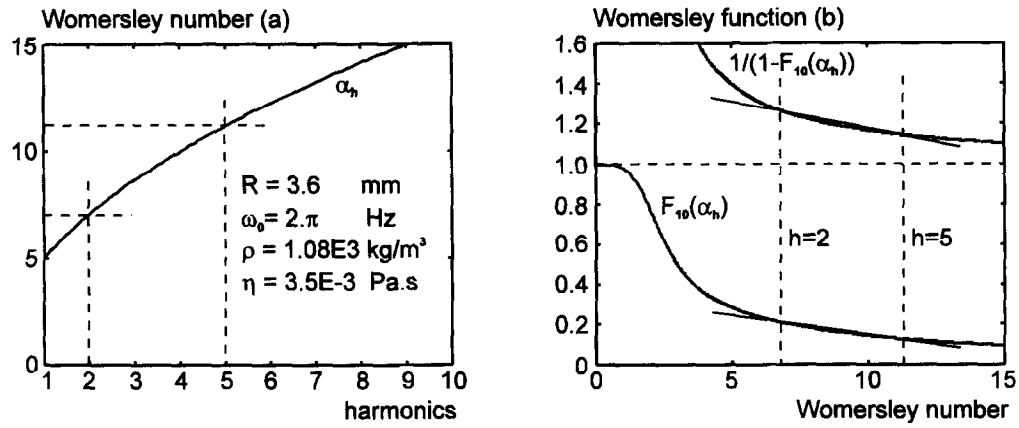

Fig. 5. (a) The Womersley number, α_h, in the common carotid artery (α_1 = 5), and (b) the real part of the function $1/(1 - F_{10}(\alpha_h))$ and the Womersley function $F_{10}(\alpha_h)$.

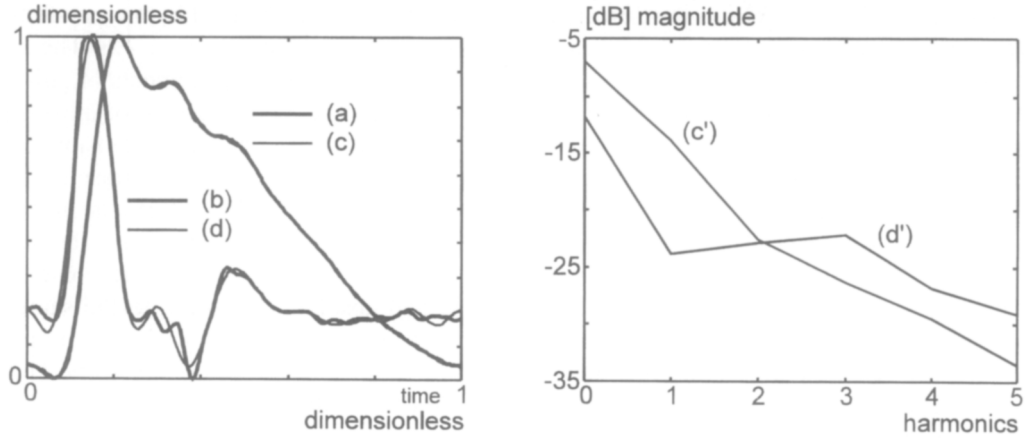

Fig. 6. The normalized distension (a) and center-line blood flow velocity (b) as measured in the common carotid artery together with six harmonics of distension (c) and center-line blood flow velocity (d) in time and frequency domain (c′) and (d′).

sound was performed through an *in vitro* study in a flow model with a distensible tube and a volume flow pulse with a Womersley number of $\alpha_1 = 15$.

The distensible tube in the *in vitro* setup (Fig. 7) is composed of two component silicone elastomers and has a length of 545 mm, an inner radius of 9 mm, a wall thickness of 1 mm and a speed of sound of 1010 m/s. The tube was installed in a closed-flow circuit with a stationary and a nonstationary pump. The stationary pump led the fluid from a reservoir to the distensible tube via a rigid inlet tube with a length of 3.75 m (200 times the tube diameter). The length of this rigid inlet tube was long enough to obtain a fully developed velocity profile at the entrance of the distensible tube. A nonstationary pump was installed between the stationary pump and the rigid inlet tube. The pulsatile pump generated a volume flow pulse ($f_0 = 1$ Hz) based on the first 10 harmonics of an aorta volume flow pulse presented by Milnor (1989). To create physiologic pressure–flow relations in the distensible tube, the tube was terminated with a hydraulic load (Fig. 7). This hydraulic load was adjusted to create a terminal impedance characteristic for the thoracic aorta. The fluid in the flow circuit was a water–glycerol mixture (40% glycerol and 60% water) containing small air bubbles (diameter of 10–30 μm) for scattering of the pulsed

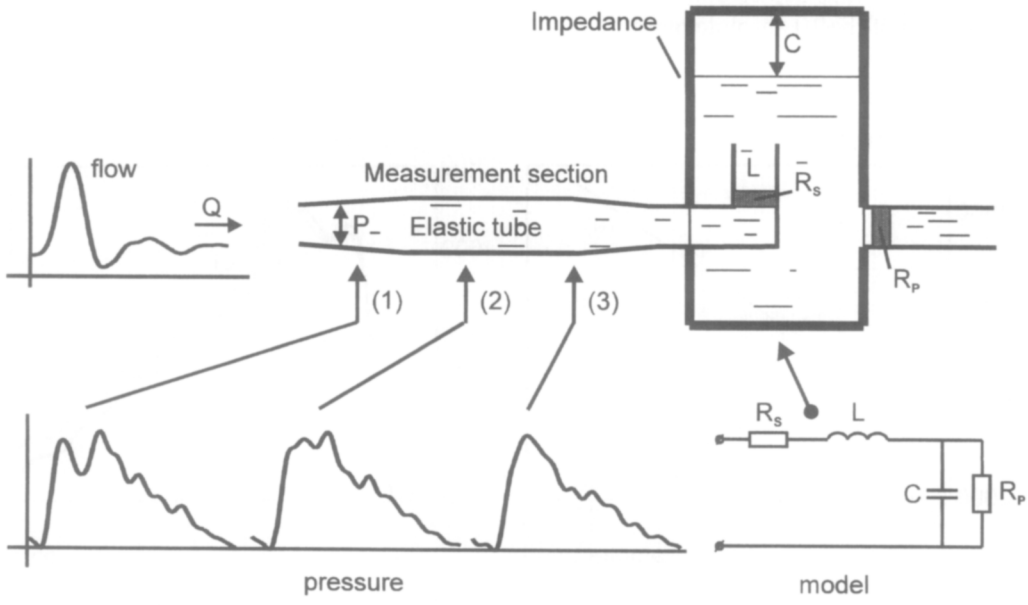

Fig. 7. Schematic diagram of the *in vitro* setup composed of a distensible tube terminated with a hydraulic load.

ultrasound. The air bubbles of 10–30 μm were created in the reservoir before the stationary pump by means of air led through a porous stone on the bottom of this reservoir. The small bubbles were led in the fluid volume flow, while the bigger bubbles surfaced in the reservoir. The fluid was Newtonian with a density of 1096 kg/m^3, a speed of sound of 1700 m/s and a dynamic viscosity of 3.4 mPa·s. Distension of the tube and center-line flow velocity inside the tube were measured at three positions (1 = 106 mm, 2 = 231 mm and 3 = 356 mm downstream from the entrance of the tube) with pulsed ultrasound. The volume flows proximal and distal to the tube were measured with electromagnetic flow probes (Skalar). The pressure in the tube was measured by means of a catheter-tip pressure transducer (Millar) at the three given positions simultaneously with distension. The local volume flow waveforms in the tube at the three positions were determined from the velocity profiles measured with laser Doppler anemometry (Fig. 7).

Validation of absolute distension

To validate the measurement of distension, absolute distension is obtained from the static pressure–diameter relation at position 2 in the distensible tube and compared with the ultrasound distension measurement (Fig. 7). Pressure was increased stepwise by increasing the volume flow. At each pressure level, the inner diameter of the tube was measured by means of laser light. In Fig. 8b, the mean values of 10 measurements of absolute and assessed pulsatile distension are shown. The absolute pulsatile distension is calculated from the pulsatile pressure waveform and the static pressure–diameter relation, as depicted in Fig. 8a. The coefficient of variation of the 10 absolute pulsatile distension curves as obtained by means of the static pressure–diameter relation was 5.2%. The coefficient of variation of the 10 measurements of pulsatile pressure was 3.5%. The normalized root-mean-square (rms) difference between absolute distension and the distension as assessed by means of ultrasound (echo system Q = 2) was 1.6%. This 1.6% is much lower than the coefficient of variation of the absolute distension because the variation in pressure contributes to pressure and absolute distension to the same extent. The time-dependent bias (Fig. 8, right) originates from the CCM estimator and was 6.6% at the end of a pump cycle (1 s). Although the bias of the CCM estimator, due to the bandwidth assumption in the derivation of this estimator (Hoeks et al. 1993), is very low, it still contains a perceptible bias because of the integration of the velocity for vessel wall displacement. The value of this bias depends on the velocity and the quality factor of the ultrasound probe. A low bias is obtained for a high quality factor ($Q > 2$), *i.e.*, a low resolution.

RESULTS

On each of the three measurement positions in the distensible tube, 10 measurements of the dimensionless reference vascular impedance and 10 measurements of the dimensionless ultrasound vascular impedance were obtained. The 10 repetitive measurements enabled estimation of the standard deviation. In Fig. 9, the results of both methods are shown. Because of the relatively high Womersley number used (α_1 = 15, a realistic value for the aorta), above the first harmonic ($h > 0$) the reference vascular impedance is almost linear with the ultrasound vascular impedance (Fig. 9). The pressure and volume flow recordings are based on ensemble averaging of 32 repetitive measurements in time,

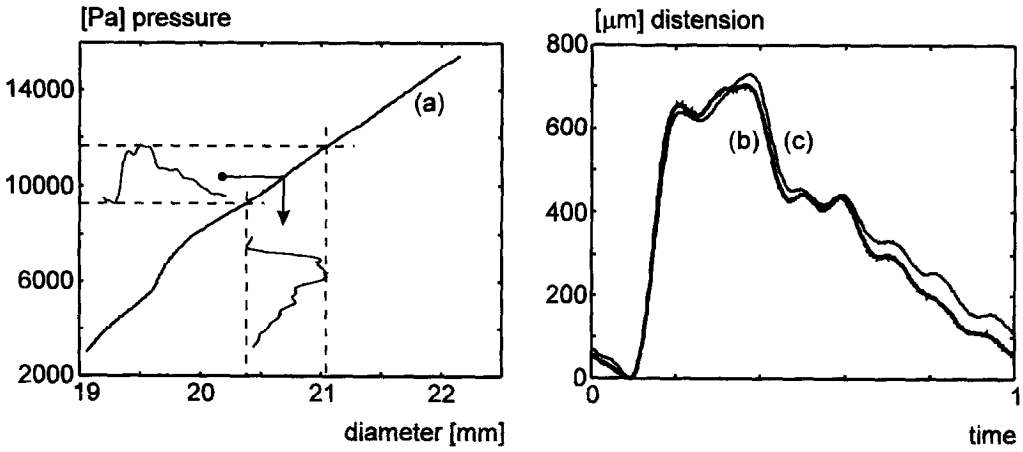

Fig. 8. The absolute distension (b) as obtained by means of the static pressure–diameter relation (a) and the distension as assessed with ultrasound (c).

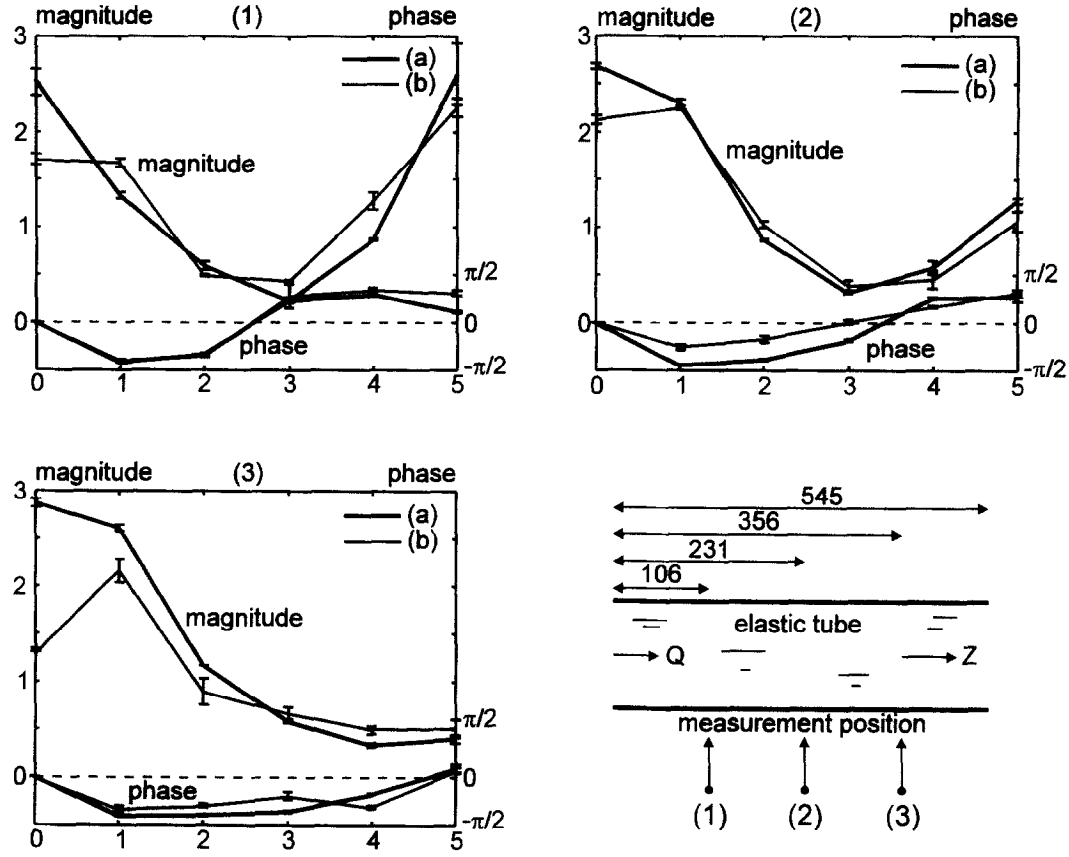

Fig. 9. The magnitude and phase of the first six harmonics of the dimensionless reference vascular impedance (a) together with the dimensionless ultrasound vascular impedance (b) at three positions downstream the entrance of the tube (1), (2) and (3).

while ultrasound distension and center-line flow velocity are based on a single recording. The normalized rms difference in magnitude between the dimensionless reference vascular impedance and the dimensionless ultrasound vascular impedance at the three positions, for the second to the fifth harmonic, was 11% (absolute ± 0.14). The normalized rms difference in phase at the three positions was 18% (absolute ± 0.016).

DISCUSSION

Despite the importance of arterial impedance to investigate heart load, distal arterial bed vasomotricity and for the quantification of the distal arterial impedance changes induced by modification of the environment, relatively few studies on vascular impedance in humans have been performed. The basic problem in the determination of vascular impedance *in vivo* pertains to the simultaneous recording at the same location of the volume flow and pressure waveforms. As an alternative, Powalowski (1989) developed a noninvasive method to estimate the vascular impedance based on simultaneous recording of distension and volume flow velocity by means of ultrasound. In the method of Powalowski (1989), the conversion from the distension waveform to the pressure waveform is based on the assumption that there is a general parametric logarithmic relation between the cross-sectional area change of the common carotid artery and the blood pressure measured in the brachial artery.

The method described in this article to obtain an estimate of the dimensionless vascular impedance in the common carotid artery is based on normalization of the distension and center-line blood flow velocity. This normalization has the advantage that it is not necessary to calibrate the blood pressure waveform using the logarithmic distension–pressure conversion with the systolic and diastolic pressure measured in the brachial artery. However, the use of normalized distension and normalized center-line blood flow velocity makes it necessary to assume a linear relationship between distension and pressure and between center-line blood flow velocity and volume flow. Moreover, due to linearization and normalization, it is impossible to estimate peripheral resistance ($h = 0$).

From the Womersley theory, it follows that the linearity between center-line blood flow velocity and volume flow depends on heart rate, radius of the vessel and viscosity of blood. The relation between these variables and the harmonics of heart rate is given by the dimensionless Womersley number. Theoretically, it follows that for a high Womersley number ($\alpha_1 > 5$, a realistic value for the common carotid artery see Fig. 5a), a pulse wave length substantially greater than the radius of the artery, a radial velocity at the wall smaller than the center-line velocity and a given range of harmonics (two to five), center-line blood flow velocity is linear with volume flow. This conclusion is supported by the results obtained in the *in vitro* experiments (Fig. 9). It is obvious that, if the distension and center-line blood flow velocity waveforms are assessed in vessels affected by atheroma, the assumed linear relationship between local distension and local blood pressure becomes invalid.

Ultrasound RF-domain signal processing allows to assess noninvasively, simultaneously and accurately the distension and center-line blood flow velocity waveforms (Hoeks et al. 1993). The ultrasound recordings are taken at an angle of 65° with the vessel axis. The angle has no effect on the dimensionless vascular impedance because of the normalization of distension and center-line blood flow velocity, but should be in the range between 60° and 70° to obtain a reliable velocity recording.

The discrimination between the scattered signal and the reverberations in the center of the lumen is obtained by means of a static high-pass filter. The cut-off frequency of this filter is set at 100 Hz according to the length of the temporal estimation window (10 ms). Instead of a higher order IIR filter, a second order IIR filter is used because this will give an optimum between the effect on the bias of the estimate and the removal of the clutter (Tysoe and Evans 1995).

The accuracy of the ultrasound vascular impedance first depends on the accuracy of the distension and center-line blood flow velocity assessment; and second, on the linearity between distension and pressure; and, finally, on the linearity between volume flow and center-line blood flow velocity for a given range of harmonics. The distension assessment is validated by means of the static relation between pressure and diameter in an elastic tube. The normalized rms difference between absolute distension and the distension as assessed with ultrasound was 1.6%. This low value confirms the high quality of distension assessment by means of ultrasound. On the other hand, the bias (over one heart cycle) between the absolute distension and the distension as assessed with ultrasound was 6.6%, which is quite a high value. Although the bias in the estimate of the vessel wall velocity is very low, integration introduces a biased estimate of distension. To prevent accumulation over more than one heart cycle, the integration of vessel wall velocity is restarted every heart cycle.

CONCLUSION

In the present study, a method is described to estimate noninvasively the dimensionless arterial impedance. The method is based on the evaluation of the spectral components of the normalized distension and center-line blood flow velocity waveforms, both obtained by ultrasound using off-line signal processing in three regions in depth (anterior vessel wall, center of the lumen, posterior vessel wall). The off-line processing is performed in the RF domain and consists of an RF domain velocity estimator preceded by a static vessel wall filter. It is demonstrated that, for the harmonics between two and five and for Womersley numbers as observed in the common carotid artery, center-line blood flow velocity is linear with volume flow. Moreover, the distension waveform is linearly related to the pressure waveform for a wide frequency range. Therefore, the spectral pressure–flow relation may be replaced by the spectral distension–velocity relation. It is concluded that, *in vitro*, for experimental considerations similar to the hemodynamic conditions in the aorta, the proposed method to estimate dimensionless ultrasound vascular impedance gives the same results as the spectral pressure–flow relation.

REFERENCES

Adamson SL, Morrow RJ, Languille BL. Side dependent effects of increases in placental vascular resistance on the umbilical arterial velocity waveform in fetal sheep. Ultrasound Med Biol 1990;16:19–27.

Arbeille P, Berson M, Achaibou F, Bodard S, Locatelli A. Vascular resistance quantification in high resistance areas using the Doppler method. Ultrasound Med Biol 1995;21:321–328.

Attinger E, Sugawara H, Navarro A, Riccetto A, Martin R. Pressure–flow relations in dog arteries. Circ Res 1966;19:230–245.

Brands PJ, Hoeks APG, Hofstra L, Reneman RS. A non-invasive method to estimate wall shear rate using ultrasound. Ultrasound Med Biol 1995;21:171–185.

De Jong PGM, Arts TGJ, Hoeks APG, Reneman RS. Determination of tissue motion velocity by correlation interpolation of pulsed ultrasonic echo signals. Ultrason Imag 1990;12:84–98.

Farrar DJ, Green HD, Bond MG, Wagner WD, Gobbee RA. Aortic pulse wave velocity, elasticity, and composition in a nonhuman primate model of atherosclerosis. Circ Res 1978;43:52–62.

Gow BS, Taylor MG. Measurements of viscoelastic properties of arteries in the living dog. Circ Res 1968;23:111–122.

Hoeks APG, Arts TGJ, Brands PJ, Reneman RS. Comparison of the performance of the RF cross-correlation and Doppler autocorrelation technique to estimate the mean velocity of simulated ultrasound signals. Ultrasound Med Biol 1993;19:727–740.

Hoeks APG, Di X, Brands PJ, Reneman RS. An effective algorithm for measuring diastolic artery diameters. Arch Acoust 1995; 20:65–76.

Maulik M, Yarlagadda P, Nathanielsz P, Figueroa J. Hemodynamic

validation of Doppler assessment of fetoplacental circulation in a sheep model system. J Ultrasound Med 1989;8:177–181.

Milnor WR. Arterial impedance as ventricular afterload. Circ Res 1975;36:232–237.

Milnor WR. Hemodynamics. 2nd edn. Baltimore: Williams & Wilkins, 1989.

O'Rourke MF. Vascular impedance: the relationship between pressure and flow. In: Arterial function in health and disease. Edinburgh: Churchill Livingstone, 1982:94–132, 185–243.

O'Rourke MF, Taylor MG. Input impedance of the systemic circulation. Circ Res 1967;20:365–380.

Powalowski T. A noninvasive ultrasonic method for vascular input impedance determination applied in diagnosis of the carotid arteries. Arch Acoust 1989;14:293–312.

Randall JE, Stacey RW. Mechanical impedance of the dog's hind leg to pulsatile blood flow. Am J Physiol 1956;187:94–98.

Tysoe C, Evans DH. Bias in mean frequency estimation of Doppler signals due to wall clutter filters. Ultrasound Med Biol 1995; 21:671–677.

Westerhof N, Elzinga G. The relation between end-diastolic volume and source impedance of the left ventricle. Arch Int Physiol Biochim 1974;82:326–329.

Westerhof N, Noordergraaf A. Arterial viscoelasticity: a generalized model effect on input impedance and wave travel in the system tree. J Biomech 1970;3:357–379.

Womersley JR. An elastic tube theory of pulse transmission and oscillatory flow in mammalian arteries. Technical report TR56-614. Wright Air Development Center, 1957.